Information Capacity of the Thumb and the Index Finger in Communication

Zhi-Hong Mao*, *Member, IEEE*, Heung-No Lee, *Member, IEEE*, Robert J. Sclabassi, *Senior Member, IEEE*, and Mingui Sun, *Senior Member, IEEE*

***Abstract*—Due to its large number of degrees of freedom and extensive connection to the brain, the human hand has been used to create channels of communication for a variety of human–machine systems. However, a fundamental question about the hand channel is still unanswered: what is its information capacity? This study aims to provide quantitative indication of effectiveness of the hand as a communication channel. We estimated that per gesture, the thumb and the index finger may deliver at most 10 and 7 bits of information, respectively. Based on this, we derived an upper bound for the information capacity of the hand in gesture-based communication: 150 b/s. Knowing this bound is critical to evaluating the potential and limitation of the hand channel for various forms of human–machine interactions.**

***Index Terms*—Hand, human–machine systems, index finger, information capacity, thumb.**

I. Introduction

THE HANDS are the chief organs for human to manipulate the environment. Their large number of mechanical degrees of freedom and massive connection to the neural system offer us tremendous flexibility to perform the skilled finger movements, ranging from the roughest to the finest, from wielding a club to playing a musical instrument. Therefore, it is very natural that the hands have been used not only to handle objects but also to create channels of communication for a variety of human-centered control systems. Hand gestures have been applied to control robotic systems, where motion commands such as left, right, forward, and backward can be encoded by hand gestures [1] (here, a hand gesture refers to a hand movement, transitioning from one hand posture to another posture). The hands have been proposed to trigger speech synthesizers that allow nonvocal people to communicate [2]. Hand gestures have also been considered to create interface devices that may replace the conventional keyboard, mouse, and joystick with improved naturalness, portability, and transmission speed [3].

Manuscript received April 6, 2008; revised July 24, 2008 and November 17, 2008. First published February 6, 2009; current version published May 22, 2009. This work was supported by the National Science Foundation (NSF) under Grant CMMI-0727256. *Asterisk indicates corresponding author.*

*Z.-H. Mao is with the Department of Electrical and Computer Engineering and the Department of Bioengineering, University of Pittsburgh, Pittsburgh, PA 15261 USA (e-mail: maozh@engr.pitt.edu).

H.-N. Lee is with the Department of Information and Communications, Gwangju Institute of Science and Technology, Buk-gu, Gwangju 500-712 Korea (e-mail: heungno@gist.ac.kr).

R. J. Sclabassi and M. Sun are with the Department of Neurological Surgery, University of Pittsburgh Medical Center, Pittsburgh, PA 15213 USA (e-mail: bobs@neuronet.pitt.edu; mrsun@neuronet.pitt.edu).

Color versions of one or more of the figures in this paper are available online at http://ieeexplore.org.

Digital Object Identifier 10.1109/TBME.2008.2011817

Although the hand offers an attractive channel of communication, a fundamental question about this channel is still unanswered: what is the information capacity of the hand in delivering control commands? Knowing this capacity will be critical to evaluating the potential as well as limitation of the hand channel in human–machine interaction. The existing studies have revealed some limited aspects of the information processing in the hand. For example, it has been estimated that in a pinch grip, the thumb and index finger together have an information processing rate of about 4.5 b/s [4]; for a skilled pianist in performance, the rate of information transmission from the visual input to the output of finger movements is about 25 b/s [5], [6]; the typical and maximal rates of information transfer via American Sign Language (ASL) (visual reception) are about 22 and 53 b/s, respectively [7], [8]. However, there has been no estimate on the information capacity of the hand in communication. This study aims to provide such an estimate, which serves as a quantitative indication of effectiveness of the hand as a communication channel.

In terms of potential impacts, the study on the hand–channel capacity can provide guidance for design of efficient and unambiguous hand gesture vocabulary for human–machine interaction. The hand gesture vocabulary can be used in robotic control [9], medical systems that serve doctors [10] and aged or handicapped people [11], and navigation and manipulation in virtual environments [12], just to name a few. Furthermore, some neurological disorders, such as Parkinson's disease, can be diagnosed on the basis of the maximum information capacity of the hand [13]. Knowing the information capacity of the hand, we will be able to find out the percentage of this capacity that humans use of their hands in normal conditions. On the basis of the data obtained in normal conditions, we can potentially diagnose some neurological disorders that affect the neural information processing for hand movements [13]. Finally, some components of the methods proposed in this study can be extended to measure effectiveness of information transmission in other human–machine and brain–machine interfaces.

II. Methods

The capacity of the hand channel depends on the maximum size of the message set encoded by hand postures (end postures of gestures) that can be delivered from the brain to the hand and can be reliably recognized. Here, we distinguish gestures only by their end postures. Although there are an infinite number of postures that we can make with the hand, the size of a message set is bounded. This is because a posture, when realized by the hand, is usually not exactly the same as the desired

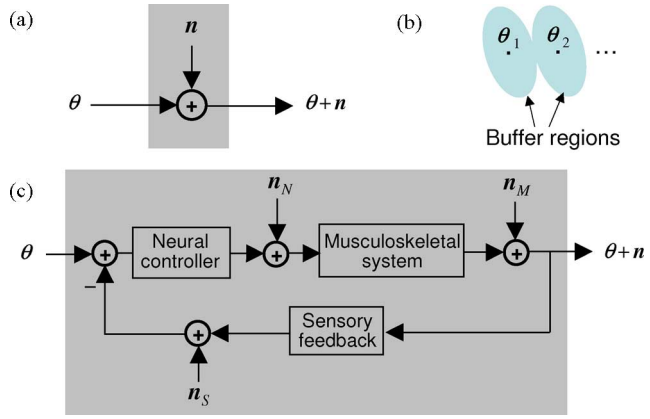

Fig. 1. (a) Conceptual model of the "hand channel." The channel input $\boldsymbol{\theta}$ is a set of parameters that characterize a posture (encoding a message) desired by the brain; $\boldsymbol{n}$ represents the noise or error imposed to the channel; and the channel output equals $\boldsymbol{\theta} + \boldsymbol{n}$, which characterizes the actual posture realized by the hand. (b) Nonoverlapping buffer regions (in a metric space of posture) for messages encoded by postures. If a received posture falls inside the buffer region of message (posture) $\boldsymbol{\theta}_i$, it implies that the posture sent by the brain is $\boldsymbol{\theta}_i$. (c) More detailed model of the hand channel with control-theoretic interpretation of the shaded area of (a). The model follows the neurocontrol architecture described in [14]. The symbols $\boldsymbol{n}_N$, $\boldsymbol{n}_M$, and $\boldsymbol{n}_S$ represent the noises or errors originated in: 1) the neural circuits that create movement command signals; 2) the musculoskeletal system; and 3) the sensory feedback system, respectively. In the steady state of gesture-making, the error in the channel output is mostly contributed from $\boldsymbol{n}_S$.

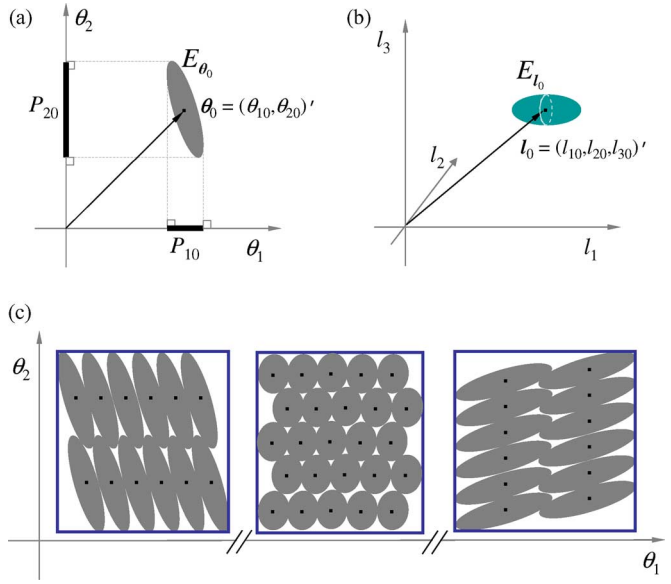

Fig. 2. (a) Joint error ellipsoid. A specific vector $\boldsymbol{\theta}_0$ in the joint angle space represents a set of joint angles $(\theta_{10}, \ldots, \theta_{m0})'$, where the prime and m represent transpose and the number of joints, respectively. For clarity, only two joint angles are shown. The ellipsoid $E_{\boldsymbol{\theta}_0}$ is an indication of the potential joint angle errors in the estimate of $\boldsymbol{\theta}_0$, and can be derived from the spindle error ellipsoid. The two intervals P_{10} and P_{20} are the projections of $\boldsymbol{\theta}_0$ on the θ_1-axis and θ_2-axis, respectively. (b) Spindle error ellipsoid. The vector $\boldsymbol{l}_0$ represents a set of muscle lengths $(l_{10}, \ldots, l_{n0})'$, which the neural system senses from the muscle spindles and which corresponds to the joint angle vector $\boldsymbol{\theta}_0$. For clarity, only three muscles are represented. Error in the estimate of $\boldsymbol{l}_0$ is characterized by an ellipsoid $E_{\boldsymbol{l}_0}$. (c) Estimation of the maximum number of unambiguous hand postures. Consider a small range of hand motion illustrated by one of the square regions in the plot, where the sizes of joint error ellipsoids are about the same for all values of $\boldsymbol{\theta}$ in the region (the sizes and orientations of joint error ellipsoids in different regions may be different). The maximum number of distinguishable hand postures within this range of motion is bounded above by the ratio of the area of the square region to the area of a typical joint error ellipsoid in the region.

posture generated in the brain but is "contaminated" by noises and perturbations in the neural and biomechanical systems (see Fig. 1). Thus, in a metric space (e.g., joint angle space) of hand postures, we need to reserve a buffer region for a message and assign every posture within this region to the given message [see Fig. 1(b)]. Then, when this message is sent, there will be a match error (or decision error) only if the received posture falls outside the buffer region. The size of the buffer region is expected to be sufficiently large so that the probability of match error is small. In such a way, the intention of the brain can be unambiguously read from the hand postures and transitions of postures.

We aim to estimate two upper bounds, denoted by N_1 and N_2, for the maximum numbers of messages that can be unambiguously encoded by the postures of the thumb and the index finger, respectively. Then, we will know that the thumb and the index finger may deliver at most $\log_2(N_1)$ and $\log_2(N_2)$ bits of information per gesture. We followed the idea of "close packing" and took two steps to estimate N_1 and N_2. The first step was to estimate the sizes of buffer regions in the joint angle space for every possible combination of joints of the thumb/index finger in posture-making. The second step was to estimate the maximum numbers of nonoverlapping buffer regions that can be contained within the whole range of joint motion of the thumb and the index finger, respectively.

A. *Step 1 (Estimate Sizes of Buffer Regions)*

We approximated a buffer region around a finger posture by an ellipsoid, called joint error ellipsoid [15], which indicates the potential joint angle error in the estimate of the given posture by the neural system. A joint error ellipsoid is a region surrounding a specific vector (or combination) of joint angles $\boldsymbol{\theta}_0$ in the hyperspace of the joint angles [see Fig. 2(a)]. The sizes of the joint error ellipsoids satisfy the following condition: two postures, represented by $\boldsymbol{\theta}_1$ and $\boldsymbol{\theta}_2$, respectively, can be sensed by the neural system to be two different postures if the two surrounding ellipsoids $E_{\boldsymbol{\theta}_1}$ and $E_{\boldsymbol{\theta}_2}$ do not overlap; otherwise, they cannot be reliably distinguished by the neural system during reproduction of these two postures from the memory.

Why can we approximate a buffer region with a joint error ellipsoid? From a control-theoretic perspective, in the steady state of gesture-making, the error between the actual posture and the brain-desired posture is mainly contributed from the sensing error in the sensory pathway rather than from the error in the movement generation pathway (see Appendix A). In other words, in the steady state, the limits of performance in hand gesturing are imposed by the position sense, not the capacity of motor realization of the target postures. This is evident from a report about people who had both a unilateral loss of position sense and impaired motor control [16], [17]: these people found it much more difficult to move the normal limb to match the position of the impaired one (mainly affected by the

sensing error) than to move the affected limb to match the normal one (mainly affected by the error in the movement generation pathway). Therefore, it is a good approximation to include only the sensing error in the error of posture-making, so we used the joint error ellipsoid of a finger posture to approximate a buffer region around the posture.

Since the sizes and orientations of joint error ellipsoids may vary significantly from posture to posture, we did not make direct measurements, but instead estimated the size of a joint error ellipsoid from a spindle error ellipsoid. We followed the general belief that the sensory feedback from muscle spindles is the primary source of the proprioceptive information about limb position [15] and derived the joint error ellipsoid from the spindle error ellipsoid in a hyperspace of appropriate dimensions (see Appendixes B–D). Note that here we did not consider the contribution of position sense from the visual system. In many applications of hand gestures, visual system is not primarily used for sensing and correcting the gestures (otherwise, the rate of gesture switching will be greatly reduced—a skilled typist will unlikely improve typing rate by looking at the fingers and keyboard).

A spindle error ellipsoid represents the error in the estimate of a specific set of muscle lengths [see Fig. 2(b)]. This concept was generalized from Biggs and Horch's conjecture about spindle error sphere [15] by taking into account the difference in spindle length sensitivity of different muscles. Such difference is due to the different distributions of spindles across muscles [18]. We assume that the spindle error ellipsoid has equal size for different combinations of muscle lengths. This assumption can be supported by an experimental finding that the sensitivity of the spindle to perturbations in forms of sinusoidal stretches (with magnitude of 1 mm) is independent of muscle length [19]. Note that not all points in a spindle error sphere correspond to feasible finger postures; these feasible combinations of finger joint angles constitute only a lower dimensional manifold in the spindle error sphere.

To estimate the size of a spindle error ellipsoid, we based our estimation on an experimental result by Clark *et al.* [20]. They estimated the target resolution at the proximal interphalangeal (PIP) joint of the index finger. Based on their findings, we derived the size of the projection, say P_{i0} in Fig. 2(a), of the joint error ellipsoid onto the PIP joint of the index finger [see (14) in Appendix D]. The size of P_{i0} was then used to estimate the size of a spindle error ellipsoid (see Appendix D).

Next, we applied a biomechanical model of index finger [21] and the data of muscle moment arms of the thumb [22] to establish the mapping from finger joint angles to lengths of related muscles, and then we were able to estimate the size of a joint error ellipsoid [see (12b) and (12c) in Appendix C].

B. Step 2 (Estimate Maximum Sizes of Message Sets)

We counted the numbers of the nonoverlapping buffer regions (approximated by joint error ellipsoids) within the whole range of joint motion of the thumb and the index finger, respectively. The whole range of joint motion of a finger can be represented by a closed region in the hyperspace of its joint angles. This closed region is contained in a hypercuboid, each edge length of which is determined by the maximum range of motion of a specific joint (see Table I). We partitioned this hypercuboid into small hypercubes so that within each hypercube, the sizes of joint error ellipsoids are approximately the same. However, the orientations and sizes of joint error ellipsoids in different hypercubes may be different. Within each hypercube, we estimated the maximum number of distinguishable postures of the finger under consideration. This number is bounded above by the ratio between the volume of the hypercube and the volume of a typical joint error ellipsoid in the cube [see Fig. 2(c)]. Finally, we added up the estimated bounds derived for all the hypercubes and arrived at an upper bound for the maximum number of distinguishable postures of the finger under consideration.

TABLE I
SLIGHTLY OVERESTIMATED RANGE OF MOTION OF THUMB AND INDEX FINGER (BASED ON [22] AND [23])

Joint	Range (degree)
Index MP (abduction)	21
Index MP (adduction)	28
Index MP (extension)	73
Index MP (flexion)	98
Index PIP (extension)	0
Index PIP (flexion)	110
Thumb CMC (abduction)	22.5
Thumb CMC (adduction)	22.5
Thumb CMC (extension)	27.5
Thumb CMC (flexion)	22.5
Thumb IP (extension)	25
Thumb IP (flexion)	65
Thumb MP (abduction)	17.5
Thumb MP (adduction)	17.5
Thumb MP (extension)	15
Thumb MP (flexion)	65

III. RESULTS

A. Sizes of Spindle Error Ellipsoids and Joint Error Ellipsoids

A spindle error ellipsoid is characterized by a scaling factor r [see (1a) in Appendix B]. We estimated that $r \approx 20$ mm [see (15) in Appendix D]. With r, we can appreciate the size of a spindle error ellipsoid: the "radius" of a spindle error ellipsoid along the axis of a muscle spindle is determined by $r/\sqrt{s_i}$, where s_i is the number of spindles in muscle i. For example, let muscle i be the abductor pollicis brevis, which has about 80 spindles, so $s_i = 80$ and $r/\sqrt{s_i} \approx 2.2$ mm. The estimated radii of the spindle error ellipsoid along the other axes of muscle lengths are presented in the right column of Table II.

Following the steps described in Appendix C, we were able to estimate the volumes of joint error ellipsoids for different combinations of joint angles of the thumb or the index finger. According to our calculation, for the thumb (five joint angles considered—see Appendix B), the volume of a joint error ellipsoid ranges from about 2.2×10^5 to 1.8×10^6 deg^5 over the whole range of joint motion. As mentioned previously, the whole range of thumb-joint motion is contained in a hypercuboid, each edge length of which is determined by the maximum range of motion of a specific thumb joint (Table I). The volume of this hypercuboid equals the product of all

TABLE II
AVERAGE NUMBERS OF SPINDLES IN MUSCLES CONTROLLING THUMB AND INDEX FINGER (ADAPTED FROM [18]) AND ESTIMATED "RADIUS" OF SPINDLE ERROR ELLIPSOID ALONG EACH AXIS

Muscle	Spindle number s_i	Estimated $r/\sqrt{s_i}$ (mm)
Abductor pollicis brevis	80	2.2
Abductor pollicis longus	78	2.3
Adductor pollicis	75	2.3
Extensor digiti communis	54.8	2.7
Extensor indicis	68	2.4
Extensor pollicis brevis	37	3.3
Extensor pollicis longus	78	2.3
First dorsal interosseous (radial+ulnar)	33.4	3.5
First lumbrical	52.8	2.8
Flexor digitorum profundus	81.5	2.2
Flexor digitorum superficialis	89	2.1
Flexor pollicis brevis	54	2.7
Flexor pollicis longus	121	1.8
Opponens pollicis	44	3.0

its edge lengths: $(22.5 + 22.5) \times (27.5 + 22.5) \times (25 + 65) \times (17.5 + 17.5) \times (15 + 65) \approx 5.8 \times 10^8$ deg^5. Similarly, we estimated that for the index finger (three joint angles considered), the volume of a joint error ellipsoid ranges from about 5.2×10^3 to 1.2×10^4 deg^3 over the whole range of joint motion. The volume of the hypercuboid containing the feasible combinations of joint angles of the index finger equals $(21 + 28) \times (73 + 98) \times (0 + 110) \approx 9.2 \times 10^5$ deg^3.

B. Information Delivered Through Thumb and Index Finger Per Gesture

Based on the calculated joint error ellipsoids and following step 2 in Section II, we estimated that the numbers of the nonoverlapping joint error ellipsoids within the whole range of joint motion of the thumb and index finger are bounded above by 1100 and 130, respectively. In other words, the maximum number of messages that can be unambiguously encoded by postures of the thumb is no greater than 1100 and that of the index finger is no greater than 130. In terms of bits of information, the neural system may deliver at most $\log_2(1100) \approx 10$ bits of information through the thumb and $\log_2(130) \approx 7$ bits of information through the index finger per use of a finger gesture. These estimates are consistent with the fact that the thumb is the most versatile and dexterous finger of the hand.

C. Information Capacities of Hand in Gesturing

Based on the aforementioned results for the thumb and the index finger, we further calculated a rough upper bound, which is 38 bits, for the maximum information that can be delivered through the whole hand per use of a gesture. Generally, the index finger is more dexterous than any one of the middle, ring, and pinky fingers, so it is reasonable for us to assume that each of the latter three fingers can deliver only a smaller number of messages per gesture than the index finger. In addition, per use of a gesture, the maximum information delivered through the hand should be less than the sum of the maximum information delivered through each finger. This is because many peripheral and central constraints significantly restrict the independence among the five fingers [24]. Therefore, the maximum information delivered through a hand posture should be less than $10 + 7 \times 4 = 38$ bits.

Taking into account the movement time, we derived that the information capacity of the hand in making gestures (transitions from posture to posture) is bounded above by 150 b/s. It was shown in [25] that by using the hand gestures defined by ASL, people fluent in fingerspelling can produce words at a rate of four letters per second. This is consistent with an experimental study [26] where the human subjects typically spelled words in ASL at a rate of three to four letters per second. Another experimental study [27] revealed that the average ASL word production rate for the tested subjects was 2.4 letters per second. Furthermore, when the size of the alphabet of hand gestures or signs becomes larger, the end postures of gestures become less distinguishable from each other, and the time (for movement and decision-making) to complete a gesture has to grow as well. So we believe 0.25 s (i.e., four gestures per second) is a reasonable lower bound of the average transition time (across all posture combinations) required for the hand to switch from one posture to another. Therefore, the information capacity of the hand in fingerspelling is bounded above by $38/0.25 \approx 150$ b/s.

IV. DISCUSSION

A. Related Studies

Information and control-theoretic approaches have been introduced in the study of human–machine interaction. In terms of information transmission rate, Fitts' law was proposed to quantify the speed accuracy tradeoff in human manual control [28]. This information-theoretic paradigm has received tremendous success in characterizing the "pointing channel" in human–machine interaction. On the other hand, it was shown from the controls perspective that Fitts' law is consistent with the closed-loop step response of a time-delayed system of the first order [29]. In our study, we followed the information-theoretic paradigm to investigate the limit of the hand channel in communication. Meanwhile, we also used control theory to interpret the constraints on the channel capacity imposed by errors in the sensory pathway and movement generation pathway (see Appendix A).

Researchers have investigated some limited aspects of information processing via the hand. For example, Balakrishnan and MacKenzie studied the information processing rate of the thumb and index finger in a pinch-grip movement [4]. They asked human subjects to hold a pressure-sensitive stylus with the thumb and index finger and perform a reciprocal point-select task involving only the joints of the thumb and index finger. The task was designed following Fitts' speed/accuracy paradigm [28], and the information processing rate of the thumb and index finger was estimated to be 4.5 b/s in the aforementioned task [4] (the information processing rate can be calculated by dividing the index of difficulty [28] of the task, measured in bits, by the movement time, measured in seconds). Quastler and Wulff investigated the information transmission in playing piano by sight (random music) [5], [30]. They used a wide range of key

numbers and encouraged the human subjects (experienced pianists) to play with very high speeds so as to obtain informational saturation. They estimated that the maximum rate of information transmission from visual input to finger movements is about 25 b/s [5]. The information transmission rate was calculated by dividing the mutual information between the visual input and action output by the movement time. The aforementioned two studies were both restricted to specific tasks of the hand, but their estimates provided lower bounds on the information capacity of the hand.

To our best knowledge, there has been no direct estimate of an upper bound of the information processing rate of the hand. A very rough upper bound can be obtained from the maximum rate of information transmission through all the nerve bundles in the arm. These nerve bundles carry all the information required for movement control of the hand. Hannula estimated that the maximum information transmission capacity of the nervous systems of the arm is about 10^7 b/s when the frequency coding method is applied [13]. Apparently, this upper bound is very conservative, because the nerve bundles in the arm undertake more responsibilities than control of hand movements. In our study, we provided a direct estimate of an upper bound of the information capacity of the "hand channel" based on calculation of spindle error ellipsoids and joint error ellipsoids.

Note that in this study, we considered only gesture-based (discontinuous) manual control and communication. Our estimation of channel capacity of the hand cannot be applied directly to continuous hand movements such as tracking and steering. However, the information delivered via continuous movements seems unlikely to exceed the information carried in discontinuous movements: it was reported in a set of continuous tracking experiments that the observed maximum rate of information transmission was 8.4 b/s [31], which is less than the maximum rates obtained under similar conditions in discontinuous tracking [32] or pointing experiments [33], 17 and 11.7 b/s, respectively. Therefore, the upper bound derived in this study may be extended for continuous movements.

B. Radii of Spindle Error Ellipsoid

Our estimated radii of the spindle error ellipsoid along different axes of muscle lengths are presented in Table II. These values (ranging from 1.8 to 3.5 mm) are much larger than 25 μm, which was considered in [15] as the potential error in neural estimate of length of one muscle due to the intrinsic "noisiness" and finite gain of spindle signals. Such a discrepancy can be explained as follows: the spindle error investigated in [15] is different from the error defined in our context. Biggs and Horch studied the sensitivity of spindles with respect to a change of muscle length [15], and spindles can still respond sensitively to stretches with amplitude as small as 25 μm [19]; in our study, however, we considered the error of spindles (and consequently, error of joint angles) distinguishable from the neural system during the reproduction of different postures from memory. It is apparently easier for the neural system to tell whether the present posture undergoes some perceivable changes than to judge matching of a reproduced posture with a posture stored in the memory. The latter task requires more information processing in the neural system, and thus, more sources of noises may affect the sizes of the spindle error ellipsoids and joint error ellipsoids.

C. Limitations of Our Study

In addition to the estimation of information capacity of the thumb and the index finger in communication, we provided an upper bound (150 b/s) for the information transmission rate of the whole hand in gesture-making. This upper bound is conservative because we did not consider the constraints that keep the five fingers from acting independently. These constraints may originate in the biomechanical structures of the hand. For example, a single muscle may be involved in the movement of several fingers simultaneously (the extensor digitorum communis has four tendons that insert into the second to fifth digits, and handles extension of the four fingers). The finger movements may also be constrained by the central control of the hand from the nervous system. The nervous system has evolved to simplify the control of multifinger movements at the price of sacrificing the flexibility of the hand. The control has been able to handle the large number of degrees of freedom during frequent and fundamental uses of the hand [24]. Due to these constraints, hand postures are restricted to some lower dimensional manifolds in the joint angle space.

D. Future Work

Considering the aforementioned constraints, we will undertake human experiments in our future study on the information capacity of the whole hand. Our proposed work is outlined in the following four steps.

Step 1: We will obtain an ergodic sampling of hand postures. This can be achieved by asking human subjects to arbitrarily create hand postures.

Step 2: We will utilize principal component analysis (PCA) to determine the dimensionality of the manifold to which the hand postures are restricted in the joint angle space (similar to the method in [34]); moreover, we will map this manifold onto a space of "primitive" postures, which has reduced dimensionality than the space of joint angles. Any hand posture can be denoted by a point in the space of the primitive postures, with coordinates representing the weights of contributions of the primitive postures in the given hand posture. Here, the idea of primitive posture decomposition is similar to that proposed in [35], where pen gesture strokes were decomposed into lower level elements.

Step 3: We will estimate the error ellipsoids in the space of primitive postures (similar to the joint error ellipsoids in the joint angle space). An error ellipsoid of a hand posture can be estimated by asking human subjects to memorize the posture and then to reproduce it repeatedly. We can calculate the mean and variance of the distribution of the repeated postures. Based on the variance model for computing target resolution [20], we can derive the size of the corresponding error ellipsoid.

Step 4: We will follow a similar method as introduced in this paper to estimate an upper bound for the maximum number of the error ellipsoids that can be packed into the region of hand postures in the space of primitive postures. Such bound is an upper bound for the maximum number of distinguishable hand postures.

V. Conclusion

In this paper, we estimated the information capacity of the thumb and the index finger in gesture-making based on the calculation of joint error ellipsoids and spindle error ellipsoids. We derived that the brain may deliver at most 10 bits of information through the thumb and 7 bits of information through the index finger per use a finger gesture. Based on this, we estimated that the information capacity of the hand in making gestures is bounded above by 150 b/s. This study provided quantitative indication of effectiveness and potential of the hand as a communication channel. In future work, we will consider the constraints imposed by the neural system on the planning and control of hand movements. The neural system has developed strategies to reduce dimensionality of the motor control, but at the same time, these strategies have sacrificed flexibility of the hand, and thus, exert limits on the information capacity of the hand. Figuring out these limits will provide us another angle to appreciate the neural strategies of movement control.

Appendix A

Approximating Buffer Regions With Joint Error Ellipsoids

In the hyperspace of joint angles of the thumb or the index finger, a *buffer region* is reserved for a finger posture (end posture of a gesture) that encodes a message. A buffer region around a finger posture can be approximated by the joint error ellipsoid of the given posture. This is because in the steady state of gesture-making, the error between the actual posture and the target posture desired by the brain is mainly contributed from the sensing error in the sensory pathway rather than from the error in the movement generation pathway. A control-theoretic justification is given in the following.

Let us examine the movement generation at a single joint, which can be modeled as a linear control system after simplification (see Fig. 3). Although the neuromuscular system is nonlinear, the linear approximation around an equilibrium is reasonable when the state variables of the system vary within a small range of that equilibrium; under situations where the system is operating beyond this small range, we may consider the linear approximation around another equilibrium. The input of the control system in Fig. 3, i.e., θ, is the angle desired by the brain at the given joint, and the output $\hat{\theta}$ is the actual joint angle realized by the finger. With the introduction of Laplace transform, a linear time-invariant analog system can be modeled as a transfer function such that the Laplace transform of the system's zero-state response equals the multiplication of the transfer function and the Laplace transform of the system input [36].

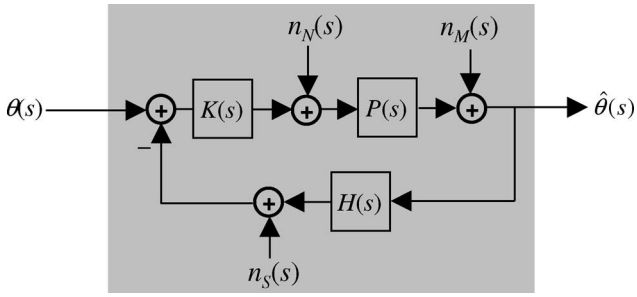

Fig. 3. Modeling the movement generation at a finger joint as a linear control system. The system input θ is the angle desired by the brain at the given joint and the output $\hat{\theta}$ is the actual joint angle realized by the finger. We use $K(s)$, $P(s)$, and $H(s)$ to represent the transfer functions for the neural controller, musculoskeletal system, and sensory feedback, respectively, and use n_N, n_M, and n_S to represent the noises or perturbations in the corresponding pathways, respectively.

The system in Fig. 3 is a single-input single-output version of Fig. 1(c). We use $K(s)$, $P(s)$, and $H(s)$ to represent the transfer functions for the neural controller, musculoskeletal system, and sensory feedback, respectively, and use $n_N(s)$, $n_M(s)$, and $n_S(s)$ to represent the Laplace transforms of the noises or perturbations in the corresponding pathways, respectively. Then, we can derive

$$\hat{\theta}(s) = \frac{K(s)P(s)\theta(s) + P(s)n_N(s) + n_M(s) - K(s)P(s)n_S(s)}{L(s)}$$

where $L(s) = 1 + K(s)P(s)H(s)$.

In the steady state, the gain of a system equals the magnitude of the system's transfer function at $s = 0$ [36]. Therefore, in the steady state

$$\hat{\theta}_{\rm ss} = \frac{K(0)P(0)\theta_{\rm ss} + P(0)n_{N\rm ss} + n_{M\rm ss} - K(0)P(0)n_{S\rm ss}}{L(0)}$$

where the subscript ss is used to indicate the steady-state value of the corresponding variable. Note that: 1) $P(0)$ should be bounded and nonzero, because bounded input to the musculoskeletal system always leads to bounded output, and the system can have an output of nontrivial steady state in response to some bounded input signal; 2) $H(0)$ should equal one, because the desired joint angle and the actual joint angle are compared in the same metric space and their units must match each other; and 3) $K(s)$ should have high gain at low frequency range, because $K(s)$ contains a component of $1/s$, i.e., neural integrator [14]—therefore, ideally, $\lim_{s\to 0} K(s) = \infty$. Based on these arguments

$$\frac{K(0)P(0)}{L(0)} = 1, \qquad \frac{P(0)}{L(0)} = 0, \qquad \frac{1}{L(0)} = 0.$$

So

$$\hat{\theta}_{\rm ss} = \theta_{\rm ss} - n_{S\rm ss}$$

which implies that under the linear-control-system approximation of the finger movement generation, the steady-state error

between the actual posture and the brain-desired posture is contributed only from the sensing error.

APPENDIX B

JOINT ERROR ELLIPSOIDS AND SPINDLE ERROR ELLIPSOIDS

Consider the hyperspace of joint angles of the thumb or index finger [see Fig. 2(a)]. Each point in that hyperspace represents a vector of joint angles: $\boldsymbol{\theta} = (\theta_1, \ldots, \theta_m)'$. For the thumb, $\boldsymbol{\theta}$ contains five joint angles for: 1) flexion/extension of the interphalangeal (IP) joint; 2) flexion/extension of the metacarpophalangeal (MP) joint; 3) abduction/adduction of the MP joint; 4) flexion/extension of the carpometacarpal (CMC) joint; and 5) abduction/adduction of the CMC joint (see Fig. 4). For the index finger, $\boldsymbol{\theta}$ contains three joint angles for: 1) flexion/extension of the PIP joint; 2) flexion/extension of the MP joint; and 3) abduction/adduction of the MP joint (see Fig. 4). Note that for the index finger, we do not consider the distal IP (DIP) joint because the motions of the DIP and PIP joints are highly dependent—during natural movements, the flexion of the DIP joint of a finger is about two-thirds of that of the PIP joint [37].

We derive the joint error ellipsoid from the spindle error ellipsoid, which takes into account the difference in spindle length sensitivity of different muscles. Such difference is due to the different distributions of spindles across muscles (see Table II).

In the hyperspace of lengths of muscles involved in the movement of the thumb or index finger [see Fig. 2(b)], each point represents a vector of muscle lengths: $\boldsymbol{l} = (l_1, \ldots, l_n)'$. For the thumb, $\boldsymbol{l}$ contains lengths of the following muscles: abductor pollicis brevis, abductor pollicis longus, adductor pollicis, extensor pollicis brevis, extensor pollicis longus, flexor pollicis brevis, flexor pollicis longus, and opponens (see Fig. 5). For the index finger, $\boldsymbol{l}$ contains lengths of extensor digitorum communis, extensor indicis, flexor digitorum profundus, flexor digitorum superficialis (FDS), first dorsal interosseous including the radial and ulnar interosseous, and first lumbrical (see Fig. 6).

For a single muscle, say muscle i stretched to an actual length of l_{i0}, the muscle length estimated by the neural system is a random variable. The error of estimation may come from a variety of sources including stochastic firing of spindles. For simplification, we approximate the error of estimation (of the length of a muscle) as a zero-mean random variable with Gaussian distribution. Following the argument of [38], the variance of this Gaussian random variable should be proportional to the reciprocal of the number of spindles in the muscle. Therefore, for muscle i, the variance of the estimation error, denoted by σ_i^2, equals σ^2/s_i, where s_i is the number of spindles in muscle i and σ^2 is the variance contributed from a single spindle.

For a set of muscles ($i = 1, \ldots, n$) with actual lengths $\boldsymbol{l}_0$, we assume that the error in the estimated length of each muscle is independent of the errors in the estimation for the others. Thus, the length vector estimated by the neural system is a Gaussian random vector, the mean of which equals $\boldsymbol{l}_0$ and the covariance matrix is a diagonal matrix: $\mathrm{diag}\{\sigma_1^2, \ldots, \sigma_n^2\} = \mathrm{diag}\{\sigma^2/s_1, \ldots, \sigma^2/s_n\}$. According to the property of level sets of a Gaussian distribution [39], for the muscles with actual lengths $\boldsymbol{l}_0$ and a fixed constant $c > 0$, the estimated muscle length vector should have the same probability density at any $\boldsymbol{l} = (l_1, \ldots, l_n)'$ on the following ellipsoid:

$$\left\{(l_1, \ldots, l_n)' \,|\, [\sqrt{s_1}(l_1 - l_{10})]^2 + \cdots + [\sqrt{s_n}(l_n - l_{n0})]^2 = c\right\}.$$

A spindle error ellipsoid $E_{\boldsymbol{l}_0}$, which surrounds a specific vector of muscle lengths $\boldsymbol{l}_0$, is then defined as follows:

$$E_{\boldsymbol{l}_0} = \Big\{(l_1, \ldots, l_n)' \,|\, [\sqrt{s_1}(l_1 - l_{10})]^2 + \cdots + [\sqrt{s_n}(l_n - l_{n0})]^2 \le r^2\Big\} \quad (1a)$$

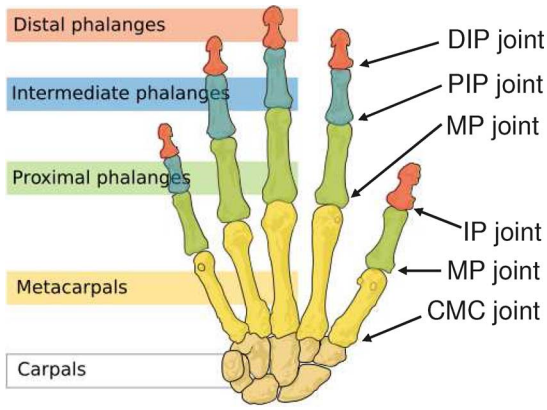

Fig. 4. Joints of the thumb and the index finger. This picture is adapted from http://commons.wikimedia.org/wiki/Image:Human_hand_bones_simple.svg.

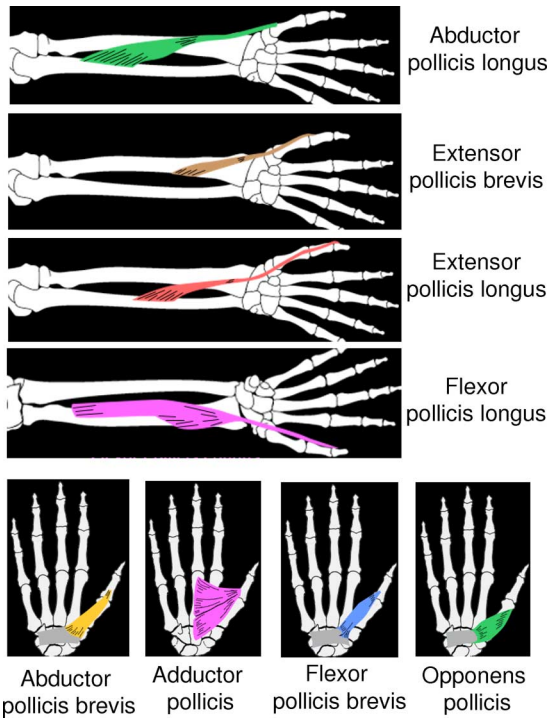

Fig. 5. Muscles controlling the movement of the thumb. This picture is adapted from http://classes.kumc.edu/sah/resources/handkines/sitemap.htm.

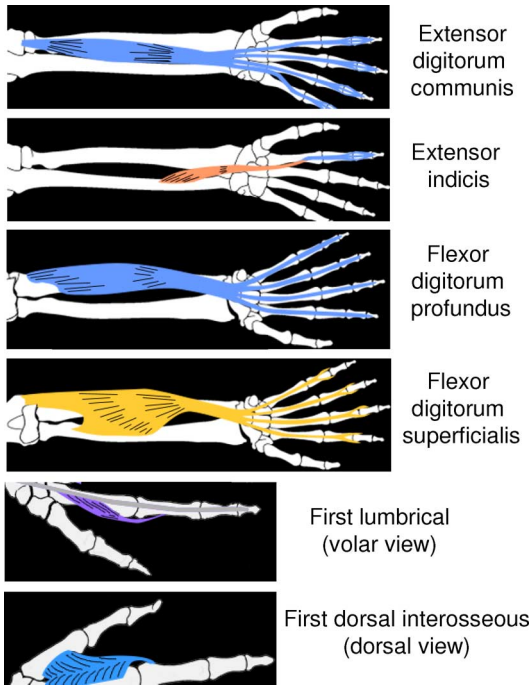

Fig. 6. Muscles controlling the movement of the index finger. This picture is adapted from http://classes.kumc.edu/sah/resources/handkines/sitemap.htm.

where r is a scaling factor characterizing the size of $E_{\boldsymbol{l}_0}$. The value of r will be estimated later in (14) and (15). In the case that s_i is the same for all i, $E_{\boldsymbol{l}_0}$ becomes a hypersphere. An equivalent expression for (1a) is

$$E_{\boldsymbol{l}_0} = \left\{\boldsymbol{l} \mid [\Lambda(\boldsymbol{l}-\boldsymbol{l}_0)]' \, [\Lambda(\boldsymbol{l}-\boldsymbol{l}_0)] \le r^2\right\} \tag{1b}$$

where

$$\Lambda = \operatorname{diag}\left\{\sqrt{s_1}, \ldots, \sqrt{s_n}\right\}. \tag{2}$$

We further assume that r does not depend on $\boldsymbol{l}_0$, i.e., $E_{\boldsymbol{l}_0}$ has equal size for different combinations of muscle lengths. As mentioned previously, this assumption can be supported by an experimental finding from [19]. In addition, the value of r should be the smallest among those that satisfy the separation criterion for spindle error ellipsoids: any two postures, represented in the hyperspace of muscle lengths by $\boldsymbol{l}_1$ and $\boldsymbol{l}_2$, respectively, can be sensed by the neural system to be two different postures during reproduction of them from memory if the two surrounding ellipsoids $E_{\boldsymbol{l}_1}$ and $E_{\boldsymbol{l}_2}$ do not overlap.

To estimate the information capacity of the thumb and the index finger in gesturing, we need to know the sizes of joint error ellipsoids. In the following, we first derive the relationship between the joint error ellipsoids and spindle error ellipsoids (see Appendix C), then estimate the sizes of spindle error ellipsoids characterized by the parameter r (see Appendix D), and finally, we can estimate the sizes of joint error ellipsoids from the value of r.

Appendix C
Estimating Joint Error Ellipsoids From Spindle Error Ellipsoids

As discussed in Section II, the error in finger joint sensation is primarily due to the error in the muscle length estimation by the neural system via the spindles. Therefore, we have the following approximated relation between the joint error ellipsoids and spindle error ellipsoids:

$$E_{\boldsymbol{\theta}_0} = \{\boldsymbol{\theta} \mid \boldsymbol{f}(\boldsymbol{\theta}) \in E_{\boldsymbol{l}_0}, \text{ where } \boldsymbol{l}_0 = \boldsymbol{f}(\boldsymbol{\theta}_0)\} \tag{3}$$

where $\boldsymbol{f} = (f_1, \ldots, f_n)'$ is a vector function that describes the relationship between muscle lengths and joint angles

$$\begin{cases} l_1 = f_1(\theta_1, \ldots, \theta_m) \\ l_2 = f_2(\theta_1, \ldots, \theta_m) \\ \quad \cdots \quad \cdots \quad \cdots \\ l_n = f_n(\theta_1, \ldots, \theta_m). \end{cases} \tag{4}$$

Consider the FDS of the index finger as an example. Sticking to the notation in Appendix B, we denote θ_1 the flexion angle of the PIP joint, θ_2 the flexion angle of the MP joint, θ_3 the adduction angle of the MP joint, and l_4 the muscle length of the FDS. Based on a biomechanical model of index finger dynamics [21], we have the following relationship between l_4 and the three joint angles:

$$\begin{aligned} l_4 &= f_4(\theta_1, \theta_2, \theta_3) \\ &= c_0 - c_1\theta_1 - c_2\theta_2 - 2c_3\left[1 - \frac{\theta_1/2}{\tan(\theta_1/2)}\right] \\ &\quad - 2c_4\left[1 - \frac{\theta_2/2}{\tan(\theta_2/2)}\right] - (c_5 + c_6\theta_3)\theta_3 \end{aligned} \tag{5}$$

where c_i $(i = 1, \ldots, 6)$ are coefficients that can be obtained from [21] ([21, eq. (4b) and Table II]), and c_0 represents the muscle length of the FDS when $\theta_1 = \theta_2 = \theta_3 = 0$. The relationship between the other muscle lengths and the joint angles of the index finger can also be obtained from [21].

In general, the dimension of $E_{\boldsymbol{l}_0}$ is greater than that of $E_{\boldsymbol{\theta}_0}$, i.e., $n > m$. In addition, not all combinations of muscle lengths correspond to feasible finger postures or feasible combinations of finger joint angles. The vector function $\boldsymbol{f}$ maps $E_{\boldsymbol{\theta}_0}$ onto a lower dimensional manifold in $E_{\boldsymbol{l}_0}$.

Since both spindle error ellipsoids and joint error ellipsoids are small, $\boldsymbol{l} = \boldsymbol{f}(\boldsymbol{\theta})$ can be approximated via linearization around $\boldsymbol{l}_0 = \boldsymbol{f}(\boldsymbol{\theta}_0)$ for $\boldsymbol{\theta} \in E_{\boldsymbol{\theta}_0}$

$$\boldsymbol{l} - \boldsymbol{l}_0 = J\,(\boldsymbol{\theta} - \boldsymbol{\theta}_0)$$

where J is an $n \times m$ Jacobian matrix defined by

$$J = \begin{bmatrix} \partial f_1/\partial\theta_1 & \cdots & \partial f_1/\partial\theta_m \\ \vdots & \ddots & \vdots \\ \partial f_n/\partial\theta_1 & \cdots & \partial f_n/\partial\theta_m \end{bmatrix}_{\boldsymbol{\theta}=\boldsymbol{\theta}_0} \tag{6}$$

where $\partial f_i/\partial\theta_j$ can be calculated from (4). For example, for the index finger

$$\frac{\partial f_4}{\partial\theta_1} = -c_1 + c_3\left[\frac{1}{\tan(\theta_1/2)} - \frac{\theta_1/2}{\sin^2(\theta_1/2)}\right]$$
$$\frac{\partial f_4}{\partial\theta_2} = -c_2 + c_4\left[\frac{1}{\tan(\theta_2/2)} - \frac{\theta_2/2}{\sin^2(\theta_2/2)}\right]$$
$$\frac{\partial f_4}{\partial\theta_3} = -c_5 - 2c_6\theta_3$$

according to (5).

The Jacobian matrix transforms changes in joint angle to changes in muscle length. The value of J depends on $\boldsymbol{\theta}_0$ and may vary as $\boldsymbol{\theta}_0$ changes.

Due to (1b) and (3), any $\boldsymbol{\theta} \in E_{\boldsymbol{\theta}_0}$ should satisfy $\{\Lambda[\boldsymbol{f}(\boldsymbol{\theta}) - \boldsymbol{l}_0]\}'\{\Lambda[\boldsymbol{f}(\boldsymbol{\theta}) - \boldsymbol{l}_0]\} \leq r^2$, which can be approximated by $[\Lambda J(\boldsymbol{\theta} - \boldsymbol{\theta}_0)]'\ [\Lambda J(\boldsymbol{\theta} - \boldsymbol{\theta}_0)] \leq r^2$. Therefore, we have the following approximation for $E_{\boldsymbol{\theta}_0}$:

$$E_{\boldsymbol{\theta}_0} = \left\{\boldsymbol{\theta} \mid [\Lambda J(\boldsymbol{\theta} - \boldsymbol{\theta}_0)]'\ [\Lambda J(\boldsymbol{\theta} - \boldsymbol{\theta}_0)] \leq r^2\right\}. \quad (7)$$

We performsingular value decomposition (SVD) [40] for the $n \times m$ matrix ΛJ, where the rank of ΛJ should be m. For ΛJ, there exists a factorization of the form

$$\Lambda J = UDV' \quad (8)$$

where U and V are $n \times m$ and $m \times m$ matrices, respectively, each of which has orthonormal columns so that $U'U = V'V = I_m$ ($m \times m$ identity matrix), and D is an $m \times m$ diagonal matrix with nonnegative numbers on the diagonal. Then

$$\begin{aligned}&[\Lambda J(\boldsymbol{\theta} - \boldsymbol{\theta}_0)]'\ [\Lambda J(\boldsymbol{\theta} - \boldsymbol{\theta}_0)]\\ &\quad = [UDV'(\boldsymbol{\theta} - \boldsymbol{\theta}_0)]'\ [UDV'(\boldsymbol{\theta} - \boldsymbol{\theta}_0)]\\ &\quad = [DV'(\boldsymbol{\theta} - \boldsymbol{\theta}_0)]'\ [DV'(\boldsymbol{\theta} - \boldsymbol{\theta}_0)].\end{aligned}$$

By introducing

$$\boldsymbol{\phi} = DV'(\boldsymbol{\theta} - \boldsymbol{\theta}_0) \quad (9)$$

which is a transformation consisting of translation, rotation, and dilation, $E_{\boldsymbol{\theta}_0}$ can be transformed into an m-dimensional hypersphere (m sphere)

$$E_{\boldsymbol{\phi}} = \left\{\boldsymbol{\phi}'\boldsymbol{\phi} \leq r^2\right\}. \quad (10)$$

According to the property of an m-sphere [41] ($m = 5$ for the thumb and $m = 3$ for the index finger—see the first paragraph of Appendix B for the m-values of the two fingers), we have

$$(\text{volume of } E_{\boldsymbol{\phi}}) \text{ for the thumb } = \frac{8}{15}\pi^2 r^5 \quad (11a)$$

$$(\text{volume of } E_{\boldsymbol{\phi}}) \text{ for the index finger } = \frac{4}{3}\pi r^3. \quad (11b)$$

According to the geometry of determinant [42], we have

$$(\text{volume of } E_{\boldsymbol{\theta}_0}) = \frac{1}{|\det(DV')|}\,(\text{volume of } E_{\boldsymbol{\phi}}).$$

Using (8), we have

$$|\det(DV')| = \sqrt{\det[(DV')'(DV')]} = \sqrt{\det[(\Lambda J)'(\Lambda J)]}$$

So

$$(\text{volume of } E_{\boldsymbol{\theta}_0}) = \frac{1}{\sqrt{\det[(\Lambda J)'(\Lambda J)]}}\,(\text{volume of } E_{\boldsymbol{\phi}}) \quad (12a)$$

$$(\text{volume of } E_{\boldsymbol{\theta}_0}) \text{ for the thumb} = \frac{8\pi^2 r^5}{15\sqrt{\det[(\Lambda J)'(\Lambda J)]}} \quad (12b)$$

$$(\text{volume of } E_{\boldsymbol{\theta}_0}) \text{ for the index finger } = \frac{4\pi r^3}{3\sqrt{\det[(\Lambda J)'(\Lambda J)]}}. \quad (12c)$$

The volume of $E_{\boldsymbol{\theta}_0}$ is a function of J, which depends on $\boldsymbol{\theta}_0$. Therefore, the size of $E_{\boldsymbol{\theta}_0}$ may vary as $\boldsymbol{\theta}_0$ changes.

Equations (12b) and (12c) show how to estimate the sizes of joint error ellipsoids for the thumb and the index finger from the sizes of spindle error ellipsoids (characterized by r). Except for r, the other parameters in (12b) and (12c) can be obtained readily: the diagonal matrix Λ is a constant matrix determined by (2); the Jacobian matrix J for the index finger can be calculated from the vector function $\boldsymbol{f}$, which is described in a biomechanical model of index finger dynamics [21]; for the thumb, J can be estimated using the data for thumb joint muscle moment arms, which is available in [22] (for a joint muscle system, the change in muscle length with respect to joint angle is the moment arm of this system). Note that the Jacobian matrix J is not constant but varies as finger posture changes. Now, the only unknown in (12b) and (12c) is r. In the following, we estimate the value of r.

APPENDIX D
ESTIMATION OF r

We take an indirect method to estimate the size of the spindle error ellipsoid, r. Our method is based on an experimental result by Clark *et al.* [20], who proposed the concept of *target resolution* to assess the exactness of position sensing. This concept can be used to estimate the maximum number of equally spaced targets that can be reliably distinguished by the neural system within a given range. Their experimental study on the PIP joint of the index finger showed that over a range of 70° (100°–170°), the resolution is 2.5 targets. In other words, a subject in their experiment could fit at most 2.5 targets (averaged over subjects) into the aforementioned range of movement at the PIP joint of the index finger, while maintaining almost error-free matching of targets when the subject tried to reproduce these targets from memory. In the following, we show how we use this result to estimate the value of r.

Generally, a joint error ellipsoid is eccentric: its projections on different axes are different. If it has larger projection on a given axis, then the joint angle represented by this axis is more difficult to estimate. The sizes of these projections can be calculated from the joint error ellipsoid. Let P_{i0} represent the projection interval of $E_{\boldsymbol{\theta}_0}$ on the θ_i-axis [see Fig. 2(a)]. It can

TABLE III
ESTIMATION OF r

Step 1: Estimate the average length of P_{i0} for the PIP joint.
Step 2: Estimate the average value of $2\sqrt{\mathbf{w}_i\mathbf{w}_i'}$ for the PIP joint.
Step 2.1: Obtain $\boldsymbol{f}(\cdot)$ in (4) based on a biomechanical model of index finger [21].
Step 2.2: For a specific combination of PIP joint angles, calculate the Jacobian matrix J using (6).
Step 2.3: Calculate Λ using (2) and Table II.
Step 2.4: Calculate D and V matrices by performing SVD upon ΛJ [see (8)].
Step 2.5: Calculate W using (13) and then the value of $2\sqrt{\mathbf{w}_i\mathbf{w}_i'}$.
Step 2.6: Repeat Steps 2.2, 2.4, and 2.5 for different combinations of PIP joint angles.
Step 2.7: Estimate the average value of $2\sqrt{\mathbf{w}_i\mathbf{w}_i'}$.
Step 3: $r \approx$ the average length of P_{i0} divided by the average value of $2\sqrt{\mathbf{w}_i\mathbf{w}_i'}$, according to (14).

be seen that

$$\text{length of } P_{i0} = \max_{\boldsymbol{\theta}\in E_{\boldsymbol{\theta}_0}} \{2(\theta_i - \theta_{i0})\}.$$

Let

$$W = (DV')^{-1} \tag{13}$$

where D and V are obtained from (8), and denote $\mathbf{w}_i$ the ith row vector of W. According to (9), we have $\theta_i - \theta_{i0} = \mathbf{w}_i\boldsymbol{\phi}$, and then

$$\text{length of } P_{i0} = \max_{\boldsymbol{\phi}'\boldsymbol{\phi}\le r^2} \{2\mathbf{w}_i\boldsymbol{\phi}\}.$$

The maximum value of the set on the right-hand side of the aforementioned expression is achieved when $\boldsymbol{\phi} = \left[\mathbf{w}_i'/\sqrt{\mathbf{w}_i\mathbf{w}_i'}\right] r$. Therefore

$$\text{length of } P_{i0} = \left(2\sqrt{\mathbf{w}_i\mathbf{w}_i'}\right) r. \tag{14}$$

Thus, the value of r can be estimated by (14) following the steps summarized in Table III. As mentioned previously, Clark *et al.* showed that within the range from 100° to 170° the target resolution of the PIP joint is about 2.5 targets [20]. This implies that the size of projection of $E_{\boldsymbol{\theta}_0}$ on the PIP joint, i.e., the length of P_{i0} in (14), is about $70/2.5 = 28°$ *on average* over a range of 70°. Next, we calculate the average value of $2\sqrt{\mathbf{w}_i\mathbf{w}_i'}$ over the same range of PIP angles (100°–170°) while setting the angle of DIP joint to be two-thirds of the PIP joint angle and fixing the flexion angle and abduction angle of the MP joint at 170° and 0°, respectively (a comfortable posture for the MP joint). Specifically, to calculate the value of $2\sqrt{\mathbf{w}_i\mathbf{w}_i'}$ for a given combination of joint angles of the index finger, we can: 1) obtain the expression for the vector function $\boldsymbol{f}$ in (4) based on a biomechanical model of index finger [21]; 2) calculate the Jacobian matrix J in (6); 3) obtain the value of Λ from (2) and Table II; 4) perform SVD upon ΛJ and get D and V matrices from (8); and 5) calculate the matrix W using (13) and the value of $\left(2\sqrt{\mathbf{w}_i\mathbf{w}_i'}\right)$. Following these steps, we compute and then average the values of $\left(2\sqrt{\mathbf{w}_i\mathbf{w}_i'}\right)$ over a set of equally spaced discrete values (5° apart from each other) of PIP joint angles within the range from 100° and 170°, and obtain the following value as an approximation for the average value of $2\sqrt{\mathbf{w}_i\mathbf{w}_i'}$: 0.0239 rad/mm or 1.37°/mm. So

$$r \approx \frac{28}{1.37} \approx 20 \text{ mm}. \tag{15}$$

ACKNOWLEDGMENT

The authors would like to thank the reviewers and editors for their valuable suggestions and comments.

REFERENCES

[1] J. Wachs, U. Kartoun, H. Stern, and Y. Edan, "Real-time hand gesture telerobotic system using the fuzzy C-means clustering," in *Proc. 5th Biannu. World Autom. Congr.*, Orlando, FL, Jun. 2002, pp. 403–409.
[2] S. S. Fels and G. Hinton, "Glove-talk: A neural network interface between a data-glove and a speech synthesizer," *IEEE Trans. Neural Netw.*, vol. 4, no. 1, pp. 2–8, Jan. 1993.
[3] V. I. Pavlovic, R. Sharma, and T. S. Huang, "Visual interpretation of hand gestures for human–computer interaction: A review," *IEEE Trans. Pattern Anal. Mach. Intell.*, vol. 19, no. 7, pp. 677–695, Jul. 1997.
[4] R. Balakrishnan and I. S. MacKenzie, "Performance differences in the fingers, wrist, and forearm in computer input control," in *Proc. ACM Conf. Hum. Factors Comput. Syst.*, Atlanta, GA, Mar. 1997, pp. 303–310.
[5] H. Quastler, Ed., *Information Theory in Psychology: Problems and Methods*. Glencoe, IL: Free Press, 1955.
[6] G. A. Miller, "Human memory and storage of information," *IRE Trans. Inf. Theory*, vol. IT-2, no. 3, pp. 129–137, Sep. 1956.
[7] C. M. Reed and N. I. Durlach, "Note on information transfer rates in human communication," *Presence: Teleoperator Virtual Environ.*, vol. 7, no. 5, pp. 509–518, Oct. 1998.
[8] S. D. Fischer, L. A. Delhorne, and C. M. Reed, "Effects of rate of presentation on the reception of American Sign Language," *J. Speech, Lang., Hear. Res.*, vol. 42, no. 3, pp. 568–582, Jun. 1999.
[9] M. Hasanuzzaman, T. Zhang, V. Ampornaramveth, and H. Ueno, "Gesture-based human–robot interaction using a knowledge-based software platform," *Ind. Robot*, vol. 33, no. 1, pp. 37–49, 2006.
[10] J. Wachs, H. Stern, Y. Edan, M. Gillam, C. Feied, M. Smith, and J. Handler, "Gestix: A doctor–computer sterile gesture interface for dynamic environments," in *Soft Computing in Industrial Applications*. Berlin, Germany: Springer-Verlag, 2007, pp. 30–39.
[11] S. P. Kang, G. Rodnay, M. Tordon, and J. Katupitiya, "A hand gesture based virtual interface for wheelchair control," in *Proc. IEEE/ASME Int. Conf. Adv. Intell. Mechatronics*, Kobe, Japan, Jul. 2003, pp. 778–783.
[12] S. Mitra and T. Acharya, "Gesture recognition: A survey," *IEEE Trans. Syst., Man, Cybern. C, Appl. Rev.*, vol. 37, no. 3, pp. 311–324, May 2007.
[13] M. Hannula, "Information transmission capacity of the nervous system of the arm—An information and communication engineering approach to the brachial plexus function," Ph.D. dissertation, Univ. Oulu, Oulu. Finland, 2003.
[14] D. Bullock, P. Cisek, and S. Grossberg, "Cortical networks for control of voluntary arm movements under variable force conditions," *Cereb. Cortex*, vol. 8, no. 1, pp. 48–62, Jan./Feb. 1998.
[15] J. Biggs and K. Horch, "Biomechanical model predicts directional tuning of spindles in finger muscles facilitates precision pinch and power grasp," *Somatosens. Motor Res.*, vol. 16, no. 3, pp. 251–262, Sep. 1999.
[16] H. Head and G. Holmes, "Sensory disturbances from cerebral lesions," *Brain*, vol. 34, pp. 102–254, 1911.
[17] L. Jones, "Dextrous hands: Human, prosthetic, and robotics," *Presence: Teleoperator Virtual Environ.*, vol. 6, no. 1, pp. 29–56, Feb. 1997.
[18] R. W. Banks, "An allometric analysis of the number of muscle spindles in mammalian skeletal muscles," *J. Anat.*, vol. 208, no. 6, pp. 753–768, Jun. 2006.
[19] T. K. Baumann and M. Hulliger, "The dependence of the response of cat spindle Ia afferents to sinusoidal stretch on the velocity of concomitant movement," *J. Physiol.*, vol. 439, pp. 320–350, Aug. 1991.
[20] F. J. Clark, K. J. Larwood, M. E. Davis, and K. A. Deffenbacher, "A metric for assessing acuity in positioning joints and limbs," *Exp. Brain Res.*, vol. 107, no. 1, pp. 73–79, Nov. 1995.
[21] N. Brooks, J. Mizrahi, M. Shoham, and J. Dayan, "A biomechanical model of index finger dynamics," *Med. Eng. Phys.*, vol. 17, no. 1, pp. 54–63, Jan. 1995.

[22] W. P. Smutz, A. Kongsayreepong, R. E. Hughes, G. Niebur, W. P. Cooney, and K. N. An, "Mechanical advantage of the thumb muscles," *J. Biomech.*, vol. 31, no. 6, pp. 565–570, Jun. 1998.
[23] R. Degeorges and C. Oberlin, "Measurement of three-joint-finger motion: Reality or fancy? A three-dimensional anatomical approach," *Surg. Radiol. Anat.*, vol. 25, no. 2, pp. 105–112, May 2003.
[24] M. H. Schieber and M. Santello, "Hand function: Peripheral and central constraints on performance," *J. Appl. Physiol.*, vol. 96, no. 6, pp. 2293–2300, Jun. 2004.
[25] R. Wolfe, N. Alba, S. Billups, M. J. Davidson, C. D. D. G. Jamrozik, L. Smallwood, K. Alkoby, L. Carhart, D. Hinkle, A. Hitt, B. Kirchman, G. Lancaster, J. McDonald, L. Semler, J. Schnepp, B. Shiver, A. Suh, and J. Young, "An improved tool for fingerspelling recognition," presented at the Technol. Persons Disabil. Conf.. Los Angeles, CA, Mar. 2006.
[26] T. E. Jerde, J. F. Soechting, and M. Flanders, "Coarticulation in fluent fingerspelling," *J. Neurosci.*, vol. 23, no. 6, pp. 2383–2393, Mar. 2003.
[27] U. Bellugi and S. Fischer, "A comparison of sign language and spoken language," *Cognition*, vol. 1, no. 2/3, pp. 173–200, 1972.
[28] P. M. Fitts, "The information capacity of the human motor system in controlling the amplitude of movement," *J. Exp. Psychol.*, vol. 47, no. 6, pp. 381–391, Jun. 1954.
[29] R. J. Jagacinski and J. M. Flach, *Control Theory for Humans: Quantitative Approaches to Modeling Performance*. Mahwah, NJ: Lawrence Erlbaum, 2003.
[30] H. Quastler and V. J. Wulff, "Human performance in information transmission," Control Syst. Lab., Univ. Illinois, Urbana, Tech. Rep. R-62, 1955.
[31] J. I. Elkind and L. T. Sprague, "Transmission of information in simple manual control systems," *IRE Trans. Hum. Factors Electron.*, vol. HFE-2, no. 1, pp. 58–60, Mar. 1961.
[32] J. C. R. Licklider, K. N. Stevens, and J. R. M. Hayes, "Studies in speech hearing and communication," Massachusetts Inst. Technol., Cambridge, MA, U.S. Air Force Contract W19 122ac-14, Final Rep., Sep. 1954.
[33] J. R. Pierce and J. E. Karlin, "Reading rates and the information rate of the human channel," *Bell Syst. Tech. J.*, vol. 36, pp. 497–516, Mar. 1957.
[34] R. Vinjamuri, M. Sun, D. Crammond, R. Sclabassi, and Z.-H. Mao, "Inherent bimanual postural synergies in hands," in *Proc. 30th Annu. Int. Conf. IEEE EMBS*, Vancouver, BC, Canada, Aug. 2008, pp. 5093–5096.
[35] X. Cao and S. Zhai, "Modeling human performance of pen stroke gestures," in *Proc. CHI Conf. Hum. Factors Comput. Syst.*, San Jose, CA, Apr./May 2007, pp. 1495–1504.
[36] C. L. Phillips and R. D. Harbor, *Feedback Control Systems*, 4th ed. Upper Saddle River, NJ: Prentice-Hall, 2000.
[37] B. Yi, F. C. Harris, L. Wang, and Y. Yan, "Real-time natural hand gestures," *Comput. Sci. Eng.*, vol. 7, no. 2, pp. 92–96, May/Jun. 2005.
[38] S. H. Scott and G. E. Loeb, "The computation of position sense from spindles in mono- and multiarticular muscles," *J. Neurosci.*, vol. 14, no. 12, pp. 7529–7540, Dec. 1994.
[39] J. A. Gubner, *Probability and Random Processes for Electrical and Computer Engineers*. Cambridge, U.K.: Cambridge Univ. Press, 2006.
[40] I. T. Jolliffe, *Principal Component Analysis*, 2nd ed. New York: Springer-Verlag, 2002.
[41] D. W. Henderson, *Experiencing Geometry in Euclidean, Spherical, and Hyperbolic Spaces*. Upper Saddle River, NJ: Prentice-Hall, 2001.
[42] K. Ito, *Encyclopedic Dictionary of Mathematics*. Cambridge, MA: MIT Press, 1993.

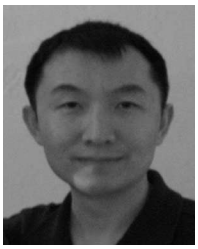

Zhi-Hong Mao (S'96–M'01) received the dual B.S. degrees in automatic control and applied mathematics and the M.Eng. degree in intelligent control and pattern recognition from Tsinghua University, Beijing, China, in 1995 and 1998, respectively, the S.M. degree in aeronautics and astronautics from Massachusetts Institute of Technology (MIT), Cambridge, in 2000, and the Ph.D. degree in electrical and medical engineering from the Harvard-MIT Division of Health Sciences and Technology, Cambridge, in 2005.

Since 2005, he has been an Assistant Professor in the Department of Electrical and Computer Engineering and the Department of Bioengineering, University of Pittsburgh, Pittsburgh, PA.

Heung-No Lee (S'94–M'99) was born in Choong-Nam, Korea. He received the B.S., M.S., and Ph.D. degrees in electrical engineering from the University of California, Los Angeles (UCLA), in 1993, 1994, and 1999, respectively.

From March 1999 to December 2001, he was with the Network Analysis and Systems Department, Information Science Laboratory, Hughes Research Laboratories, Malibu, CA, where he led a number of research projects as the Principal Investigator including traffic modeling for tactical Internet (under the Defense Advanced Research Projects Agency (DARPA) Advanced Technology Office (ATO) Adaptive Signal Processing and Networks (ASPEN) Program), future tactical networking system, capacity analysis for satellite networks using realistic input traffic, and broadband wireless modem. In 2002, he joined the Department Electrical Engineering, University of Pittsburgh, Pittsburgh, PA. Since January 2009, he has been an Associate Professor in the Department of Information and Communications, Gwangju Institute of Science and Technology, Korea. His current research interests include information and signal processing theories for wireless network and biomedical applications.

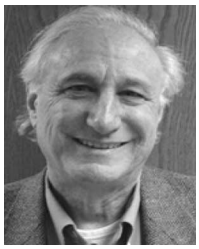

Robert J. Sclabassi (M'62–SM'93) received the B.S.E. degree in electrical engineering from Loyola University, Los Angeles, CA, the M.S.E.E. and Ph.D. degrees in electrical engineering from the University of Southern California, Los Angeles, and the M.D. degree in medicine from the University of Pittsburgh, Pittsburgh, PA.

He was with the Advanced Systems Laboratory, TRW, Inc., Los Angeles, and a Postdoctoral Fellow at the Brain Research Institute, University of California, Los Angeles (UCLA), where was also with the faculty of the Department of Neurology and Biomathematics. He is currently a Professor of neurological surgery, psychiatry, electrical engineering, mechanical engineering, and behavioral neuroscience at the University of Pittsburgh. He has authored or coauthored more than 400 papers, chapters, and conference proceedings.

Prof. Sclabassi is a Registered Professional Engineer.

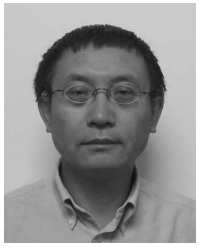

Mingui Sun (S'88–M'89–SM'05) received the B.S. degree from Shenyang Chemical Engineering Institute, Shenyang, China, in 1982, and the M.S. and Ph.D. degrees in electrical engineering from the University of Pittsburgh, Pittsburgh, PA, in 1986 and 1989, respectively.

In 1991, he joined the University of Pittsburgh, where he is currently a Professor of neurosurgery, electrical and computer engineering, and bioengineering. He is also the Director of Research at Computational Diagnostics, Inc., Pittsburgh. His current research interests include advanced biomedical electronic devices, biomedical signal and image processing, sensors and transducers, biomedical instruments, artificial neural networks, wavelet transforms, time–frequency analysis, and the inverse problem of neurophysiological signals. He has authored or coauthored more than 200 publications.